PAUL BUEHLER

Methods for automated conversion of SREM count rates to particle fluxes

Document No	:	ESTEC contract No. 19336/05/NL/Ja/pg, WP 30
Issue	:	2.0
Date	:	April 30, 2007

Dr. Paul Bühler
Auhofstrasse 22/3
1130 Vienna
Austria

Contents

List of Reference Documents

[Bühler, 1996] P. Bühler, Scientific data extraction, Part I, *Report on ESTEC/Contract No. 11108/94/N1/JG(SC), WP 33, 331, 332*, December 1996

[Höcker & Kartvelishvili, 1996] A. Höcker and V. Kartvelishvili, *Nucl.Instrum.Meth.* A372 (1996) 469-481

[Bühler et al., 1998] Technical note on WP 81, *Report on ESTEC/Contract No. 11108/94/N1/JG(SC), WP 33, 331, 332*, May 1998

[Bühler et al., 1999] Energy and spatial dependence of the east-west effect observed by Mir-REM, *Space Radiation Environment Workshop, Nov. 1999, DERA, UK*

1 Introduction

This documents contains:

- review of count rate to flux conversion methods for SREM
- discussion of the application of the different methods for an automated processing of the SREM data

The document is divided into the two parts

- Theoretical considerations
- Practical considerations

2 Theoretical considerations

2.1 Relation between count rates and incident particle fluxes

The count rate c_i in counter i is related to the incident particle fluxes $f_q(E)$ (q represents ambient charged particle species) by equation (1). $RF_{i,q}(E)$ is the energy dependent response function of the counter i to incident particles q of energy E.

$$c_i = \sum_{q=p^+,e^-,...} \left[\int_0^\infty f_q(E) \cdot RF_{i,q}(E) \cdot dE \right];\ i = 1..15 \tag{1}$$

Assumption:

Contributions to c_i, from particles other than electrons and protons can be treated as background (here represented by bkg_i).

$$c_i = \sum_{q=p^+,e^-} \left[\int_0^\infty f_q(E) \cdot RF_{i,q}(E) \cdot dE \right] + bkg_i;\ i = 1..15 \tag{2}$$

Generally bkg_i is a function of time and place. Its has to be determined for each mission separately. For the following it is assumed that bkg_i is known and can be subtracted from c_i such that equation (1) finally becomes

$$c_i = \sum_{q=p^+,e^-} \left[\int_0^\infty f_q(E) \cdot RF_{i,q}(E) \cdot dE \right];\ i = 1..15 \tag{3}$$

where now the c_i represent the background corrected count rates.

2.2 Solving the basic set of equations

The equations (3) are Fredholm integral equations of the first kind. They are used to deduce the incident particle spectra from the measured count rates. However, generally these equations do not have a unique solution and approximations must be applied.

In the following possible treatments of the problem are outlined.

2.2.1 Parametrization of particle fluxes

Smooth functions

In this method the unknown incident particle fluxes are approximated by a parametric form $\mathcal{F}(\alpha, E)$ with the vector α of free parameters.

$$f_q(E) = \mathcal{F}(\alpha, E) \tag{4}$$

Using equation (3) the expected count rate $c^{th}(\alpha)_i$ can be computed, and together with c_i these are used to compute χ^2.

$$\chi^2(\alpha) = \sum_i \frac{(c_i - c^{th}(\alpha)_i)^2}{c_i} \tag{5}$$

χ^2 is a measure for the similarity of the measured c_i and computed $c^{th}(\alpha)_i$. The set of parameters α is determined for which χ^2 is minimized.

Possible spectral forms:

Power law $\mathcal{F}(\alpha, E) = f(E_0) \cdot \left(\frac{E}{E_0}\right)^{-\gamma}$
Exponential function $\mathcal{F}(\alpha, E) = f(E_0) \cdot \exp(-\gamma \cdot (E - E_0))$
Rigidity function
Broken power law

Step function

The incident spectra are approximated by a step like function. They are split into N_p (protons) and N_e (electrons) energy ranges, and the flux is assumed to be constant within each of the bins.

$$f_q(E) = \begin{cases} 0 & ; \quad E < E_{q,1} \\ f_{q,1} & ; \quad E_{q,1} < E < E_{q,2} \\ & . \\ & . \\ f_{q,N_q} & ; \quad E_{q,N} < E < E_{q,N_q+1} \\ 0 & ; \quad E > E_{q,N_q+1} \end{cases} \tag{6}$$

Inserting equation (6) into equation (3) results in

$$\begin{aligned} c_i &= \sum_m f_{p,m} \cdot \int_{E_{p,m}}^{E_{p,m+1}} RF_{i,p}(E) \cdot dE + \sum_n f_{e,n} \cdot \int_{E_{e,n}}^{E_{e,n+1}} RF_{i,e}(E) \cdot dE \\ &= \mathcal{RF} \times \{\overline{f_p}, \overline{f_e}\} \end{aligned} \tag{7}$$

$\mathcal{RF}$ is a $(N_p + N_e) \times 15$-element matrix and $\{\overline{f_p}, \overline{f_e}\}$ is a vector consisting of the $(N_p + N_e)$ flux levels.

The set of linear equations (7) can be used to compute the flux levels $\{\overline{f_p}, \overline{f_e}\}$.

2.2.2 Simple Conversion Factor SCF

This method works if only one particle species contributes to the measured count rates or if the contribution of other species is known and can be subtracted from the measurement. In the following we assume that,

$$c_i = \int_0^\infty f_q(E) \cdot RF_{i,q}(E) \cdot dE \tag{8}$$

with q either protons or electrons.

We are now seeking for a factor SCF such that

$$SCF_{i,q} \cdot c_i = \int_{E_{min,i,q}}^{E_{max,i,q}} f_q(E) \cdot dE \tag{9}$$

Combining equations (3) and (9) results in

$$SCF_{i,q} = \frac{\int_{E_{min,i,q}}^{E_{max,i,q}} f_q(E) \cdot dE}{\int_0^\infty f_q(E) \cdot RF_{i,q}(E) \cdot dE} \tag{10}$$

$SCF_{i,q}$ is obviously a function of the incident spectrum $f_q(E)$. However, if $RF_{i,q}(E)$ can be approximated by a boxcar function

$$RF_{i,q}(E) = \begin{cases} 0 & ; \quad E < E_{min,i,q} \\ RF_{i,q} & ; \quad E_{min,i,q} < E < E_{max,i,q} \\ 0 & ; \quad E > E_{max,i,q} \end{cases} \tag{11}$$

then, equation (10) becomes

$$SCF_{i,q} = \frac{1}{RF_{i,q}} \tag{12}$$

It now remains to determine the energies $E_{min,i,q}$, $E_{max,i,q}$, and the value $RF_{i,q}$ which best represent the response function $RF_{i,q}(E)$.

3 Practical considerations

3.1 Simple Conversion Factor SCF

3.1.1 Selection of counters suited for the SCF-method

The SCF-method is expected to give reliable results if the response function of a counter can be reasonably well approximated by a boxcar function. The $RF_{i,q}(E)$ of the SREM aboard Integral displayed in Figures 1 (protons) and 2 (electrons) indicate, that such an approximation may not be equally valid for all counters and needs to be investigated carefully.

Protons

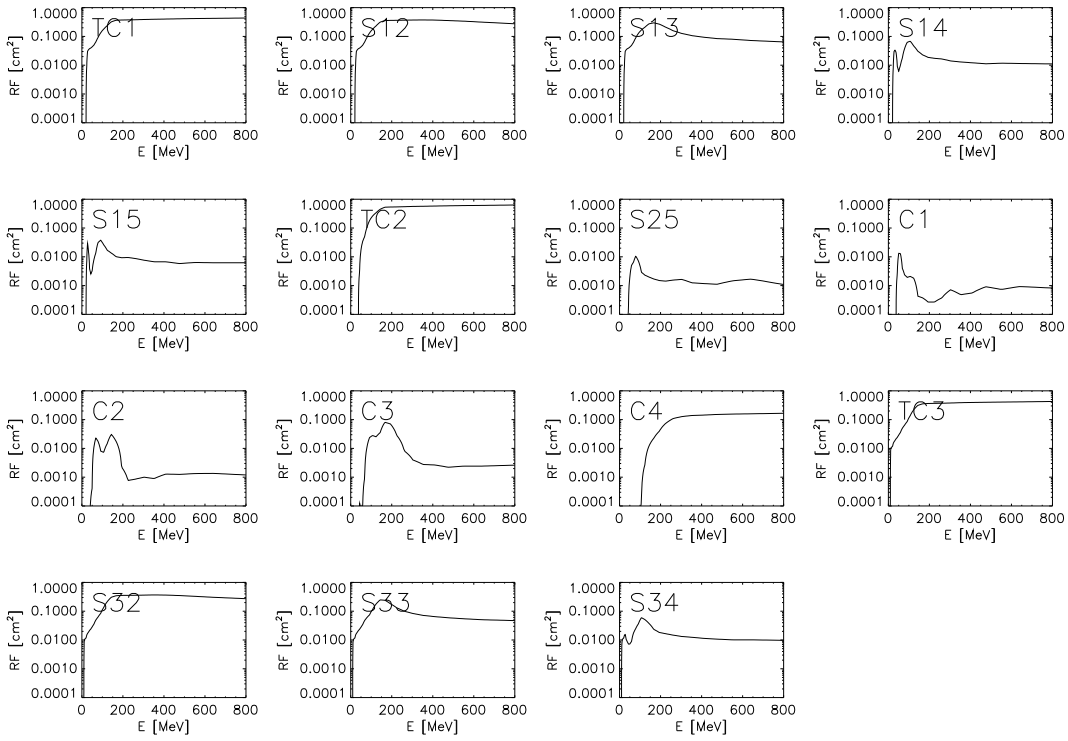

Figure 1: $RF_{i,p}(E)$ of the IREM counters

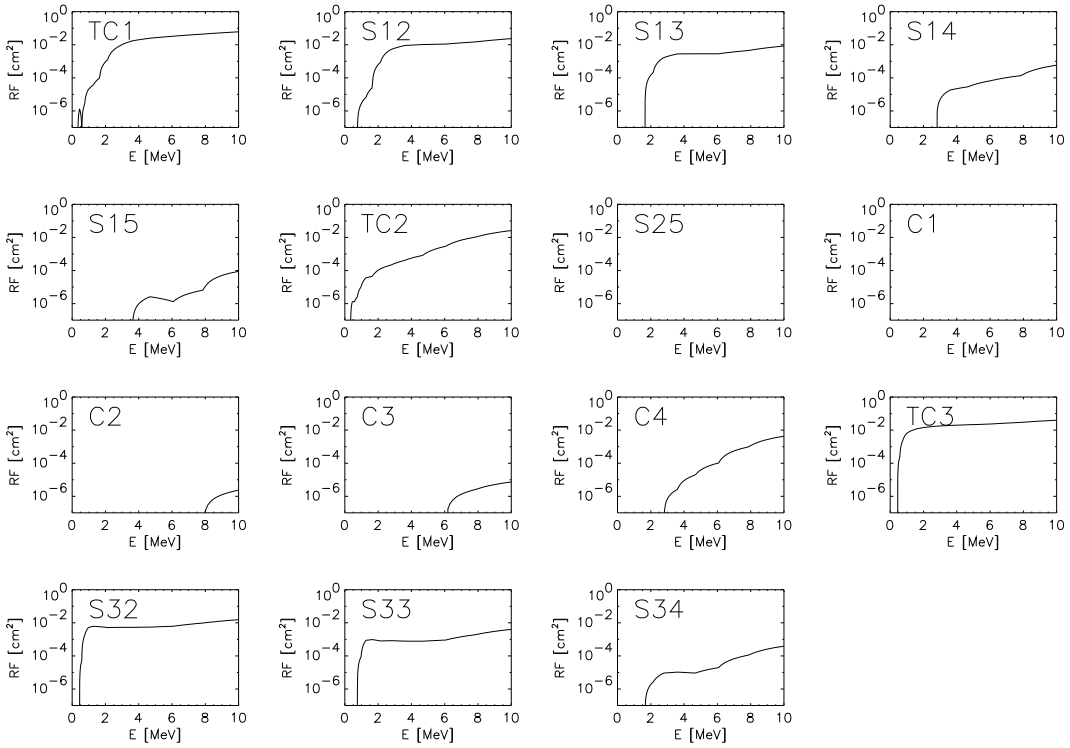

Figure 2: $RF_{i,e}(E)$ of the IREM counters

3.1.2 Computation of average SCF

Generally $SCF_{i,q}$ is a function of the shape of the incident particle spectrum and the energy limits $E_{min,i,q}$, $E_{max,i,q}$ (see equation (10)). Therefore the $SCF_{i,q}$ was computed for a range of spectral shapes and values of $E_{min,i,q}$, $E_{max,i,q}$.

For the computation of the $SCF_{i,q}$, power law and exponential functions were used with a wide range of spectral indices γ as well as a range of energy limits $E_{min,i,q}$ and $E_{max,i,q}$. The spectral parameters as well as the energy limits were varied from min to max in steps of Δ as given in Table 1. Thus for each counter and particle species 1292832 (protons) or 15200 (electrons) different combinations of γ, E_{min} and E_{max} were used to compute SCF. For the electrons E_{max} was kept constant at ∞. This simplification is motivated by the shape of the RF for electrons, which up to 10 MeV is for all counters a growing function of energy (see Figure **??**).

Among the different energy limits the two values (in case of electrons the one value) were selected for which the variation of SCF as function of spectral shape at fixed energy limits was minimized. Finally the such selected SCFs were averaged to give the final SCF value. The results are listed in Tables 2 (protons) and 3 (electrons) for IREM and Tables 4 and 5 for PROBA-1/SREM. The values STDV(SCF)/SCF represents the relative standard deviation of SCF computed for fixed energy limits (not over all SCF values).

Table 1: Range of spectral shapes and energy limits $E_{min/max}$ used for computation of SCF

protons, $E_0 = 10\ MeV$			electrons, $E_0 = 1\ MeV$		
min	max	Δ	min	max	Δ
γ, power law					
0.5	8.5	0.5	2.0	6.5	0.25
γ, exponential function					
0.01	0.41	0.025	1.5	6.5	0.25
$E_{min,i,q}$					
10	210	1	0.3	10.275	0.025
$E_{max,i,q}$					
50	850	4	$E_{max} = \infty$		

In Figures 3 to 7 the SCFs computed with the selected energy limits are plotted as function of the spectral shape. The first 16 points from left in each panel (first 18 points in case of electrons) were computed with the power law spectra, the remaining points with the exponential functions.

There are a few counters for which the approximation of RF with a boxcar function seems to be reasonable good. For these cases the dependency of SCF on the particle spectral shape is small.

For the protons this are especially counters $s14(04)$, $s15(05)$, $c1(08)$, and $s34(15)$. For counters $c3(10)$ and $c4(11)$ the SCF is rather independent of the spectral hardness of a power law spectrum, but seems to strongly depend on the spectral hardness of the exponential spectra. However, these two counters are interesting because they provide proton fluxes at high energies ($E > 80\ MeV$ and $E > 160\ MeV$). More analysis is needed to fully understand this behavior.

In case of the electrons the best behaving counters are $s12(02)$, $s13(03)$, $s14(04)$, $tc3(12)$, $s32(13)$, and $s33(14)$. For counter $s15(05)$, similar to the counter $c3(10)$ and $c4(11)$ in the case of protons, the SCF varies only little with changing spectral hardness of a power law spectrum, but decreases strongly with softening exponential spectrum. For the electrons this is a interesting counter because it provides information on the very energetic electrons ($E > 8\ MeV$).

Table 2: IREM proton SCF for various counters

cnt		E1	E2	$SCF\ [1/cm^2]$	$\frac{\text{STDV}(SCF)}{SCF}$
protons					
1	tc1	27.00	∞	15.83	0.274
2	s12	26.00	∞	19.00	0.263
3	s13	27.00	∞	16.00	0.256
4	s14	24.00	542.00	38.49	0.038
5	s15	23.00	434.00	65.62	0.057
6	tc2	49.00	∞	13.10	0.504
7	s25	48.00	270.00	208.80	0.108
8	c1	43.00	86.00	107.22	0.060
9	c2	52.00	278.00	75.63	0.133
10	c3	76.00	450.00	35.14	0.145
11	c4	164.00	∞	10.42	0.157
12	tc3	12.00	∞	49.29	0.394
13	s32	12.00	∞	49.34	0.390
14	s33	12.00	∞	40.17	0.318
15	s34	12.00	∞	63.78	0.103

Table 3: IREM electron SCF for various counters

cnt		E1	E2	$SCF\ [1/cm^2]$	$\frac{\text{STDV}(SCF)}{SCF}$
protons					
1	tc1	2.00	∞	117.96	0.370
2	s12	2.08	∞	194.62	0.293
3	s13	2.23	∞	518.92	0.211
4	s14	3.20	∞	25402.99	0.479
5	s15	8.18	∞	5460.37	0.072
6	tc2	2.80	∞	191.46	0.877
11	c4	8.10	∞	154.61	0.041
12	tc3	0.80	∞	100.72	0.116
13	s32	0.75	∞	189.47	0.044
14	s33	1.05	∞	1162.18	0.059
15	s34	2.08	∞	93077.70	0.437

Table 4: PROBA1/SREM proton SCF for various counters

cnt		E1	E2	SCF $[1/cm^2]$	$\frac{\text{STDV}(SCF)}{SCF}$
protons					
1	tc1	26.00	∞	21.15	0.308
2	s12	26.00	∞	21.28	0.300
3	s13	26.00	∞	22.22	0.233
4	s14	24.00	566.00	43.79	0.073
5	s15	22.00	646.00	88.26	0.062
6	tc2	49.00	∞	16.62	0.486
7	s25	53.00	318.00	209.40	0.144
8	c1	42.00	114.00	128.97	0.040
9	c2	51.00	270.00	91.42	0.149
10	c3	73.00	418.00	51.75	0.124
11	c4	154.00	∞	17.03	0.109
12	tc3	12.00	∞	56.63	0.205
13	s32	12.00	∞	56.87	0.202
14	s33	12.00	∞	57.35	0.207
15	s34	11.00	∞	86.13	0.140

Table 5: PROBA1/SREM electron SCF for various counters

cnt		E1	E2	SCF $[1/cm^2]$	$\frac{\text{STDV}(SCF)}{SCF}$
protons					
1	tc1	2.00	∞	169.01	0.449
2	s12	2.03	∞	361.09	0.280
3	s13	2.13	∞	1053.33	0.242
4	s14	2.73	∞	86026.21	0.518
5	s15	8.18	∞	8451.06	0.226
6	tc2	3.10	∞	174.70	1.092
11	c4	7.75	∞	216.37	0.045
12	tc3	0.80	∞	203.36	0.159
13	s32	0.73	∞	438.66	0.076
14	s33	1.03	∞	2198.48	0.076
15	s34	1.98	∞	171428.90	0.440

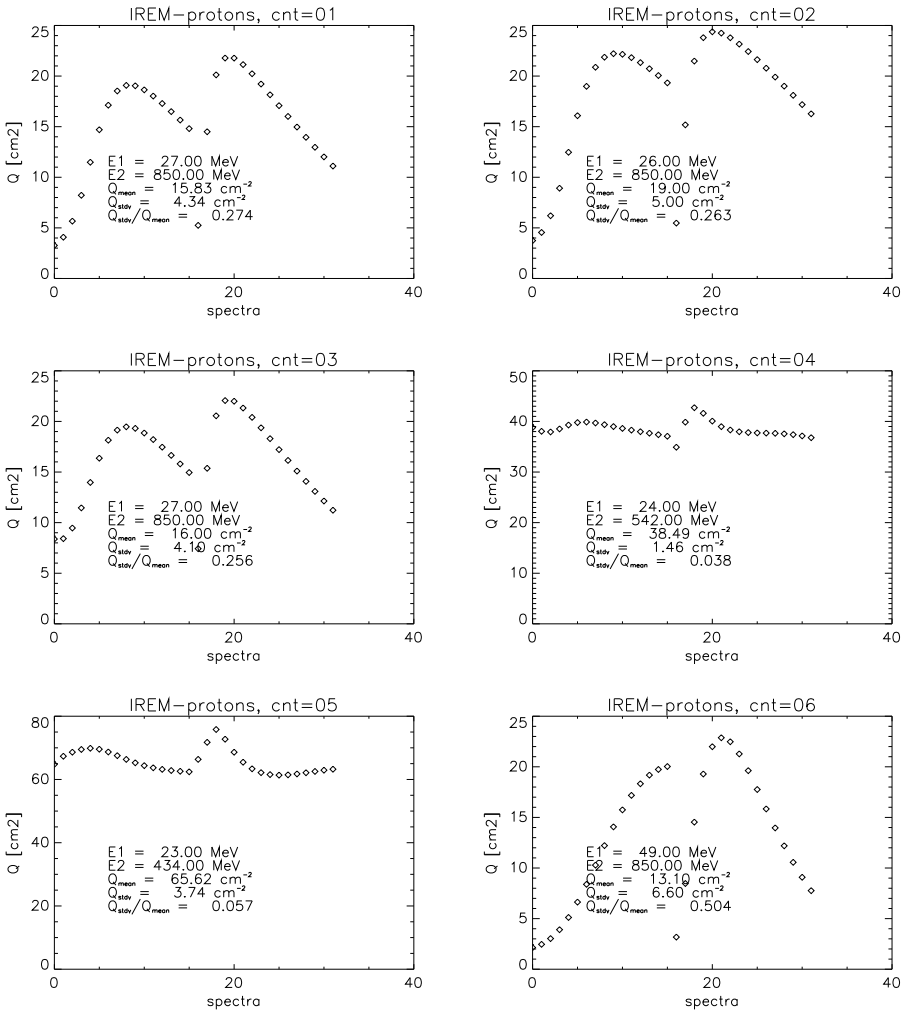

Figure 3: SCF for protons computed with equation (10) for the spectral shapes listed in table 1. The first 16 points (starting from left) are computed with power law spectral shapes, the remaining points, with exponential functions.

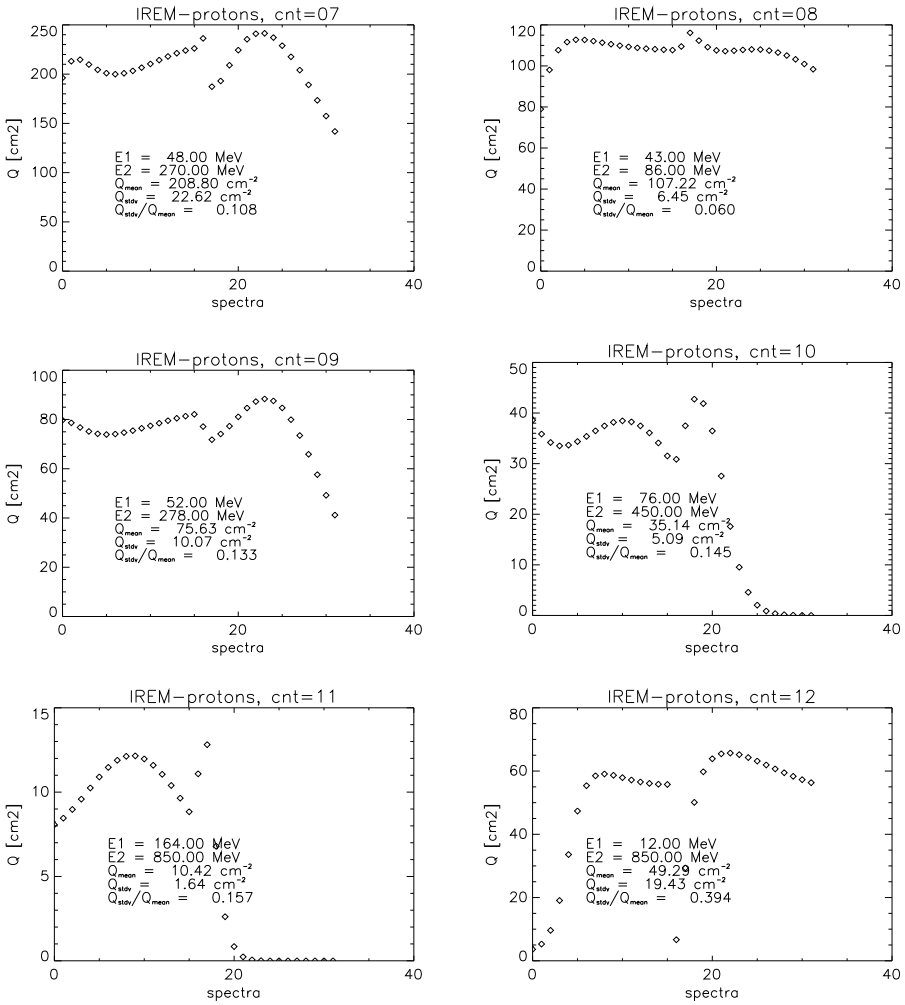

Figure 4: Same as figure 3 but for other counters.

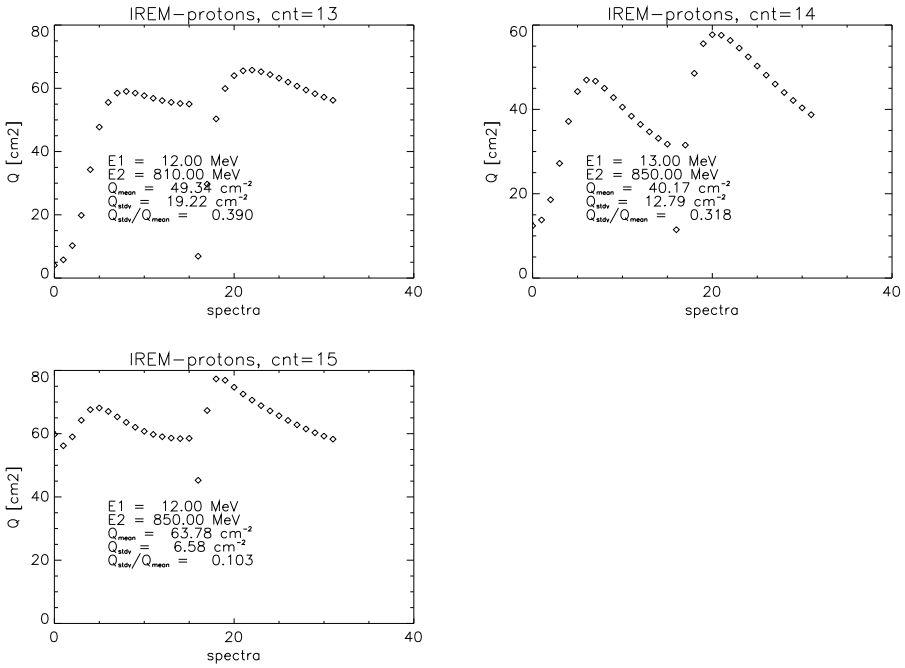

Figure 5: Same as figure 3 but for other counters.

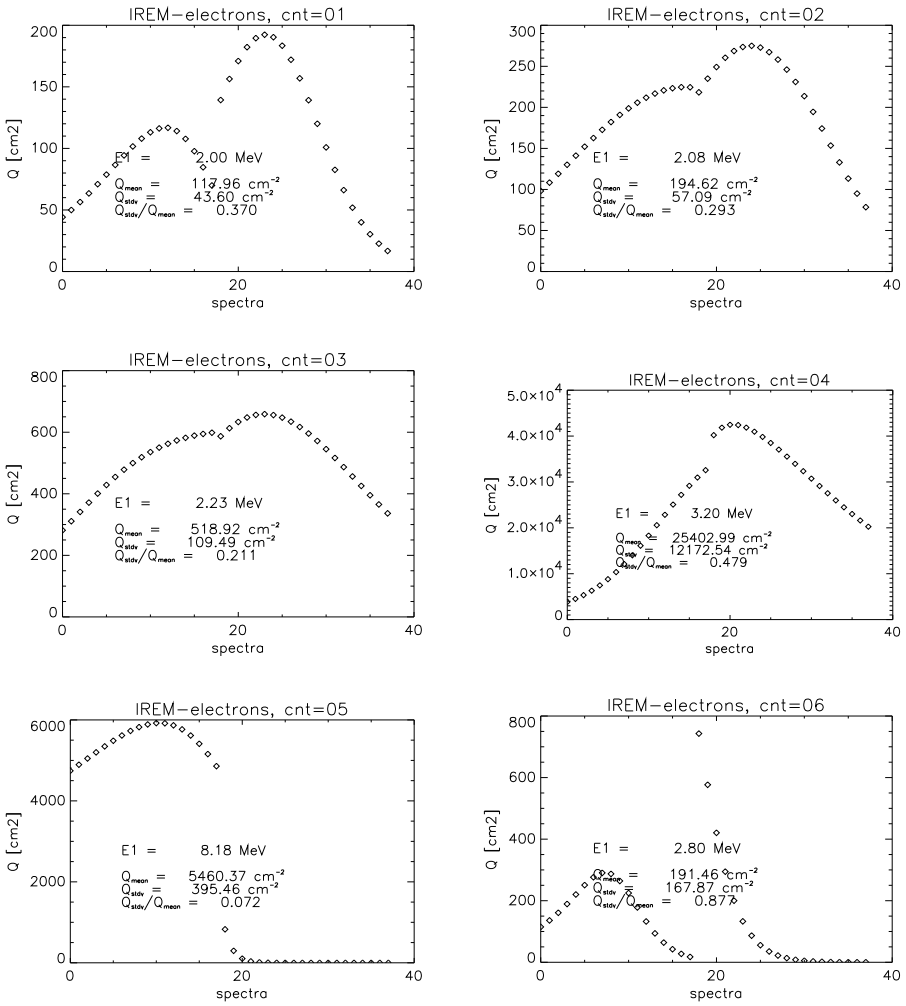

Figure 6: SCF for electrons computed with equation (10) for the spectral shapes listed in Table 1. The first 19 points (starting from left) are computed with power law spectral shapes, the remaining points, with exponential functions.

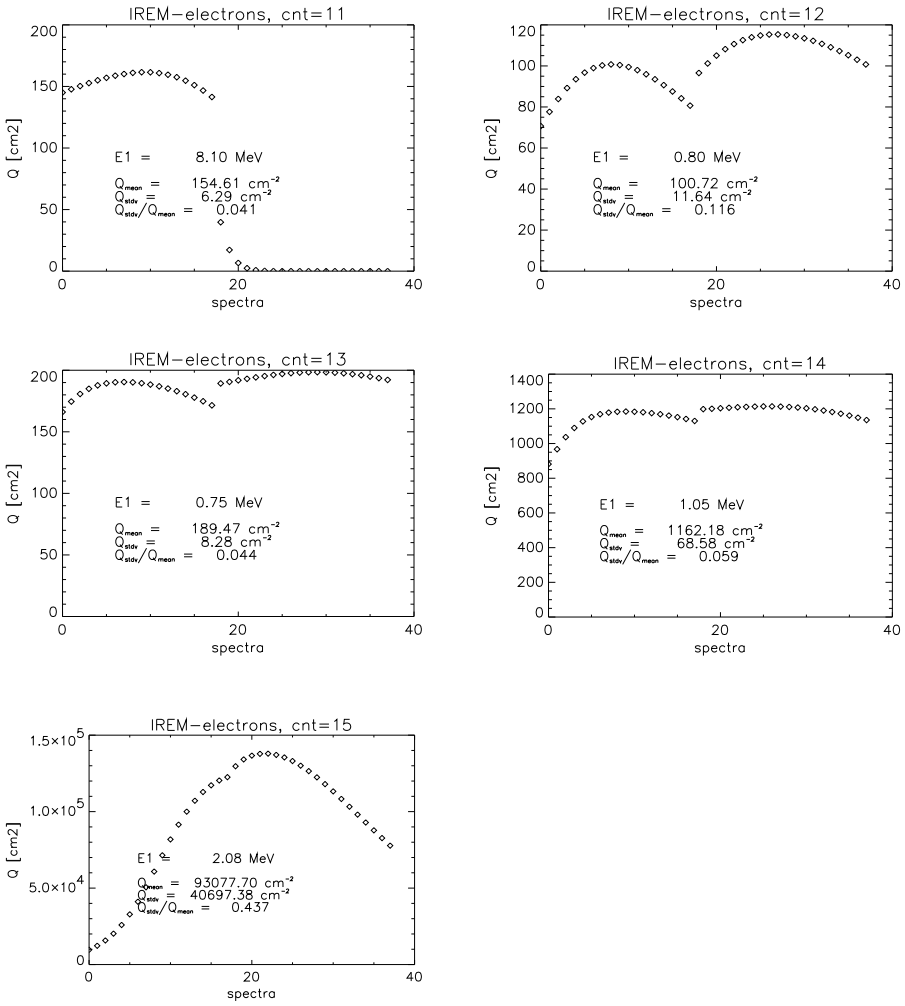

Figure 7: Same as figure 6 but for other counters.

3.1.3 Flowcharts for conversion with SCF

The SCF-method consists of three steps:

1. decide which particle species is dominant
2. decide whether counter is contaminated with other particle species
3. convert count rates with appropriate SCF

Counter ratios can be used to determine the dominating particle species and contaminations. The procedure is summarized in the following flowcharts for selected counters.

Protons, #15

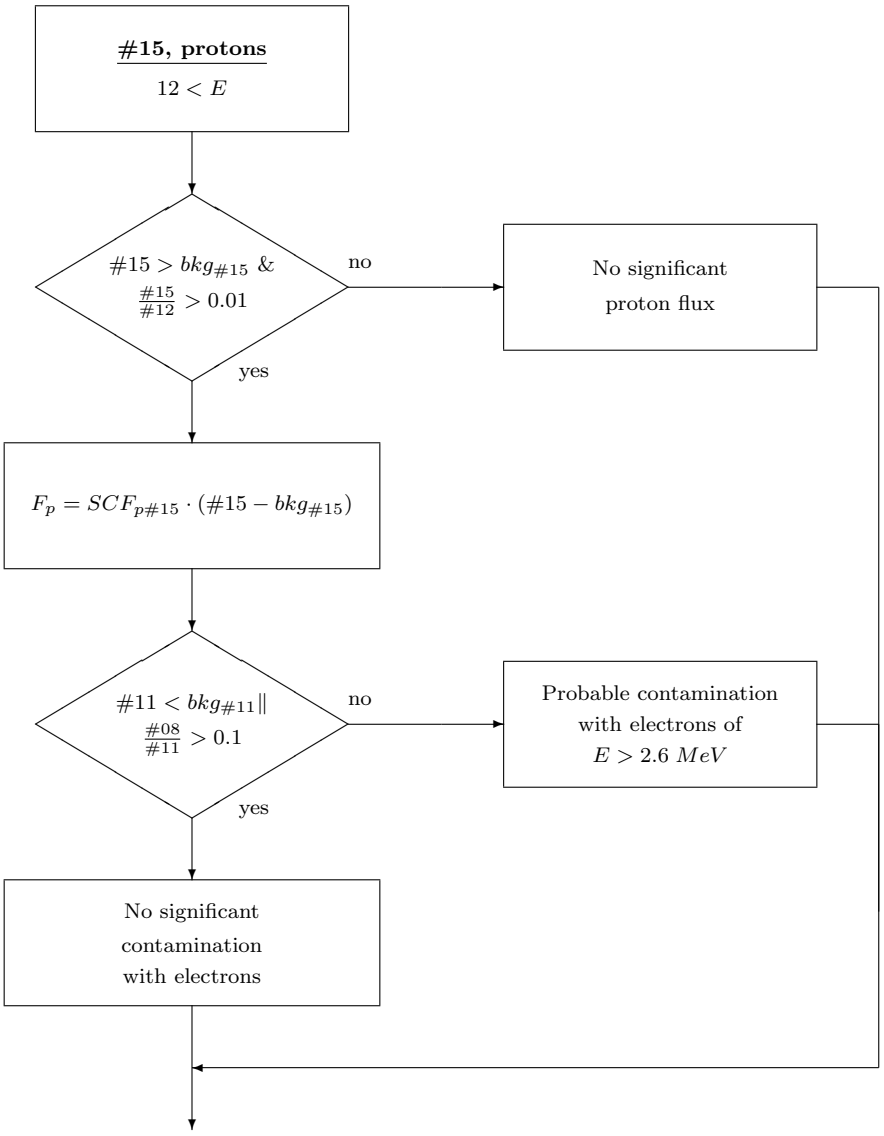

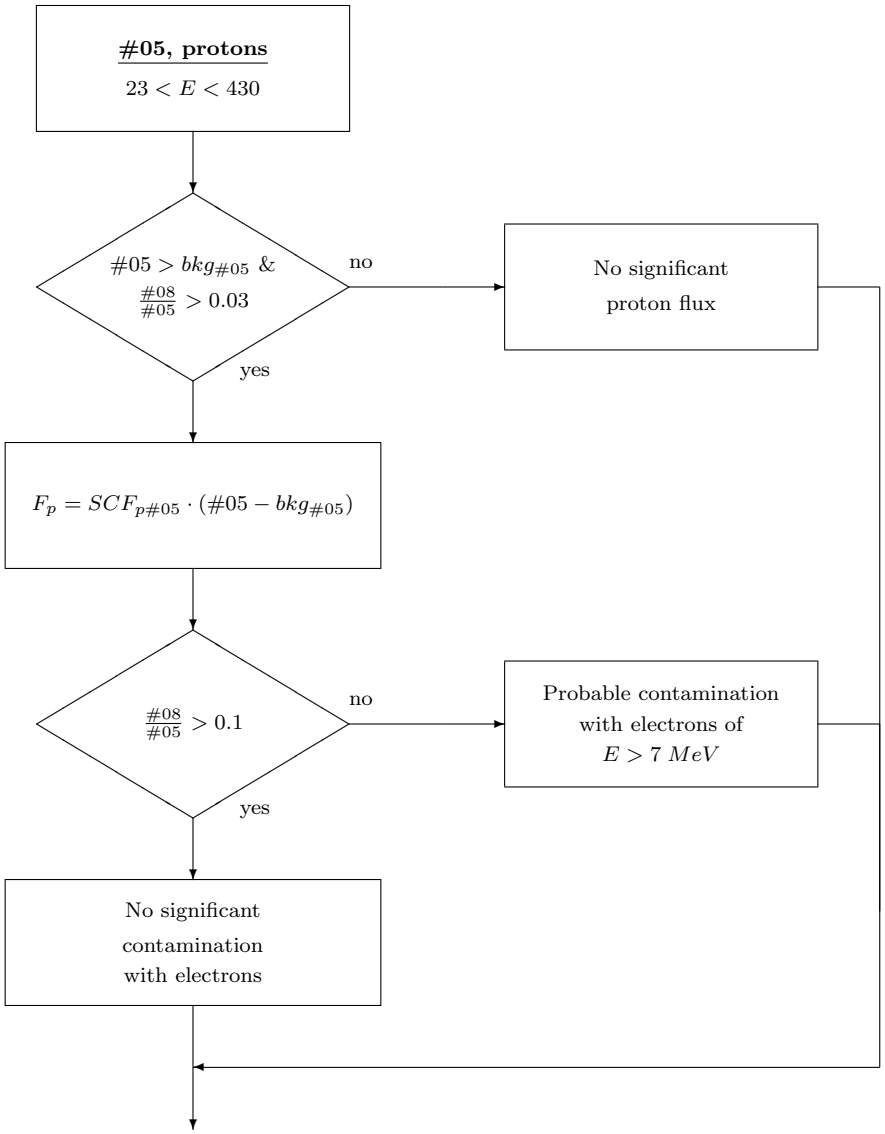
#05, protons
$23 < E < 430$
$\#05 > bkg_{\#05}$ & $\frac{\#08}{\#05} > 0.03$
no
No significant proton flux
yes
$F_p = SCF_{p\#05} \cdot (\#05 - bkg_{\#05})$
$\frac{\#08}{\#05} > 0.1$
no
Probable contamination with electrons of $E > 7\ MeV$
yes
No significant contamination with electrons

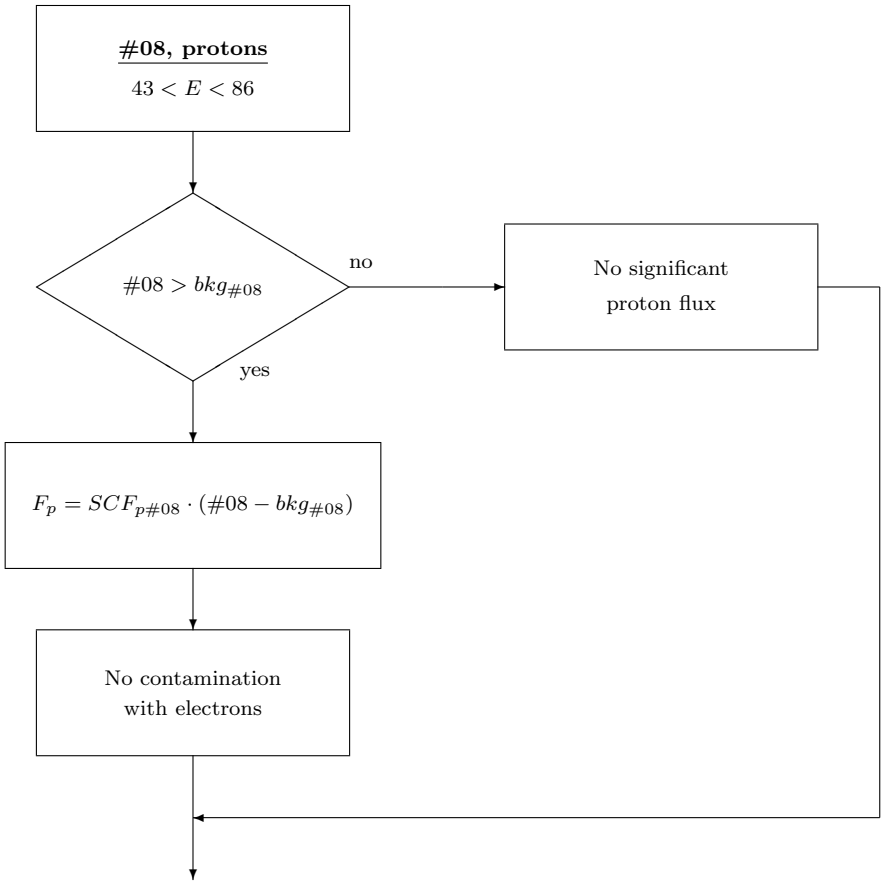
#08, protons
$43 < E < 86$
$\#08 > bkg_{\#08}$
no
yes
No significant proton flux
$F_p = SCF_{p\#08} \cdot (\#08 - bkg_{\#08})$
No contamination with electrons

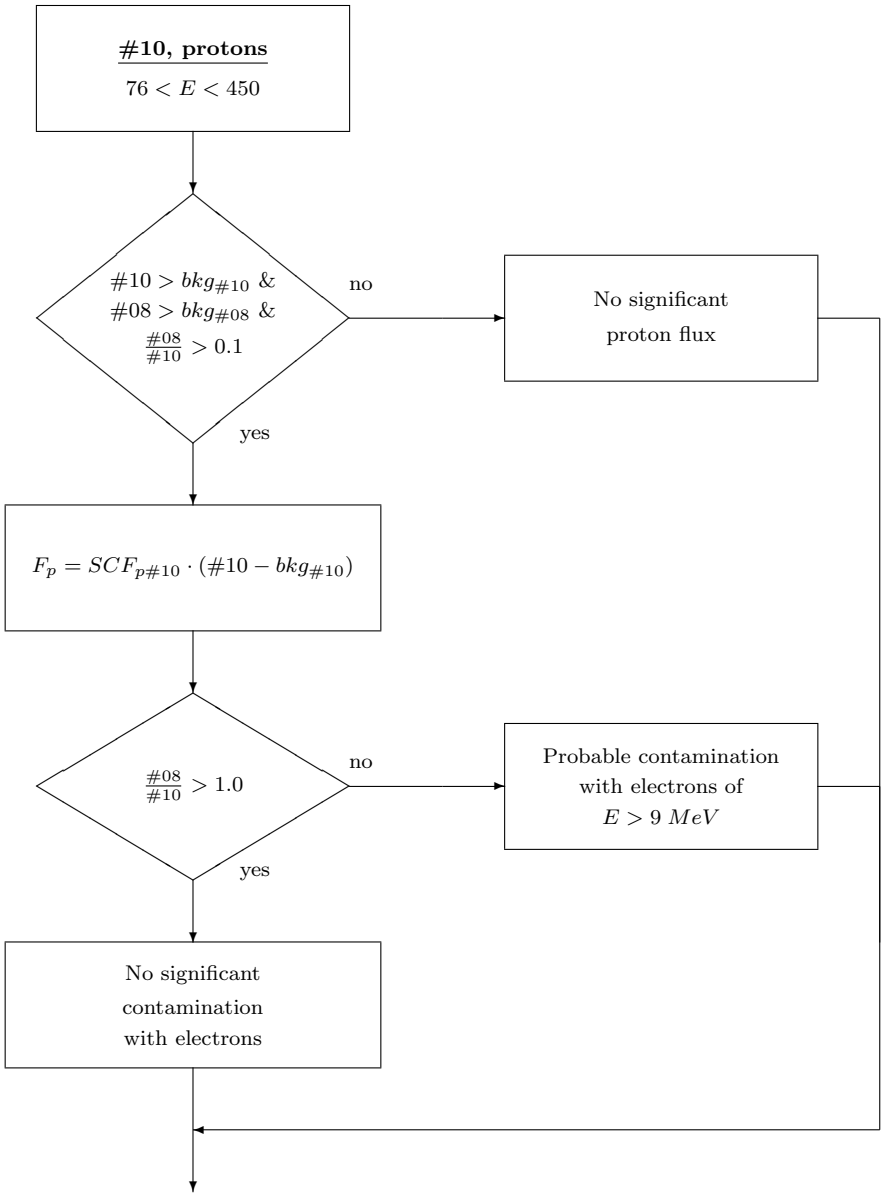
#10, protons
$76 < E < 450$
$\#10 > bkg_{\#10}$ &
$\#08 > bkg_{\#08}$ &
$\frac{\#08}{\#10} > 0.1$
no
No significant proton flux
yes
$F_p = SCF_{p\#10} \cdot (\#10 - bkg_{\#10})$
$\frac{\#08}{\#10} > 1.0$
no
Probable contamination with electrons of $E > 9\ MeV$
yes
No significant contamination with electrons

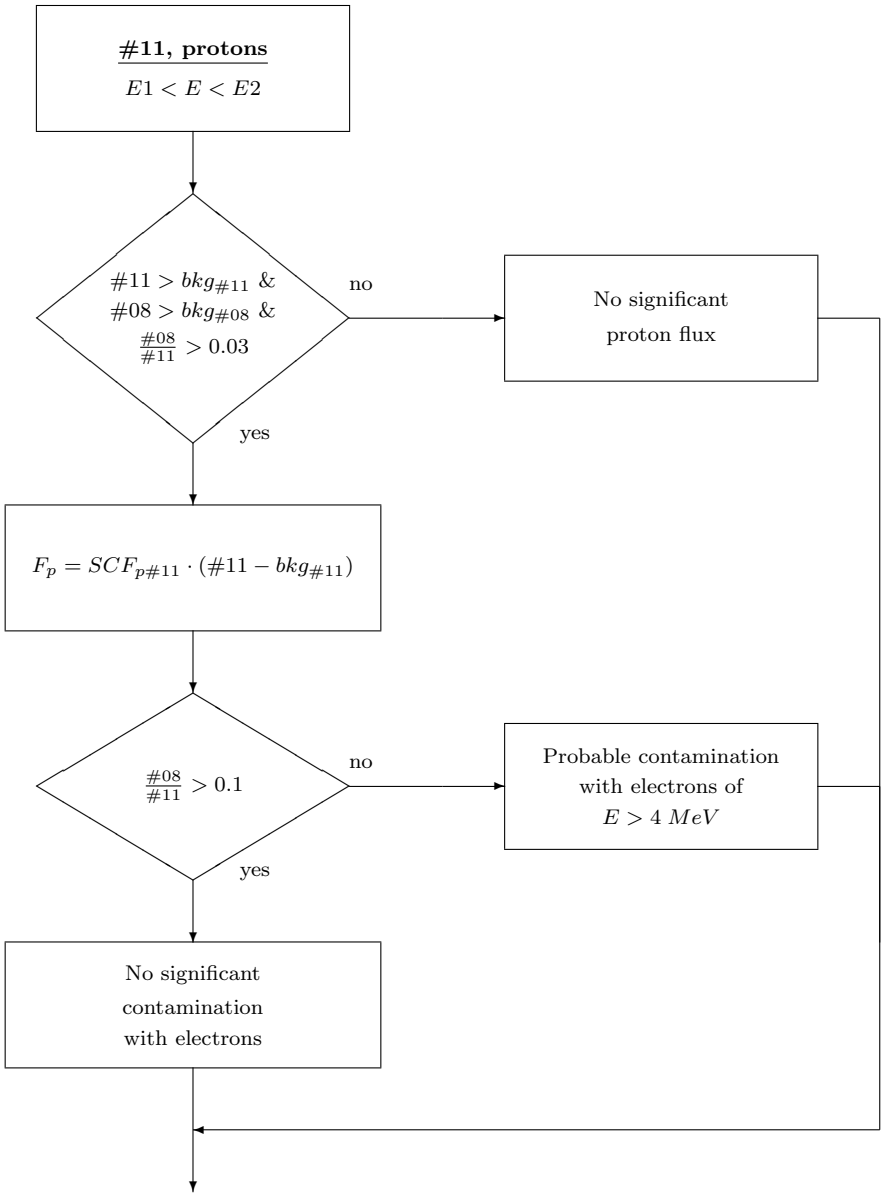
#11, protons
$E1 < E < E2$
$\#11 > bkg_{\#11}$ &
$\#08 > bkg_{\#08}$ &
$\frac{\#08}{\#11} > 0.03$
no
No significant proton flux
yes
$F_p = SCF_{p\#11} \cdot (\#11 - bkg_{\#11})$
$\frac{\#08}{\#11} > 0.1$
no
Probable contamination with electrons of $E > 4\ MeV$
yes
No significant contamination with electrons

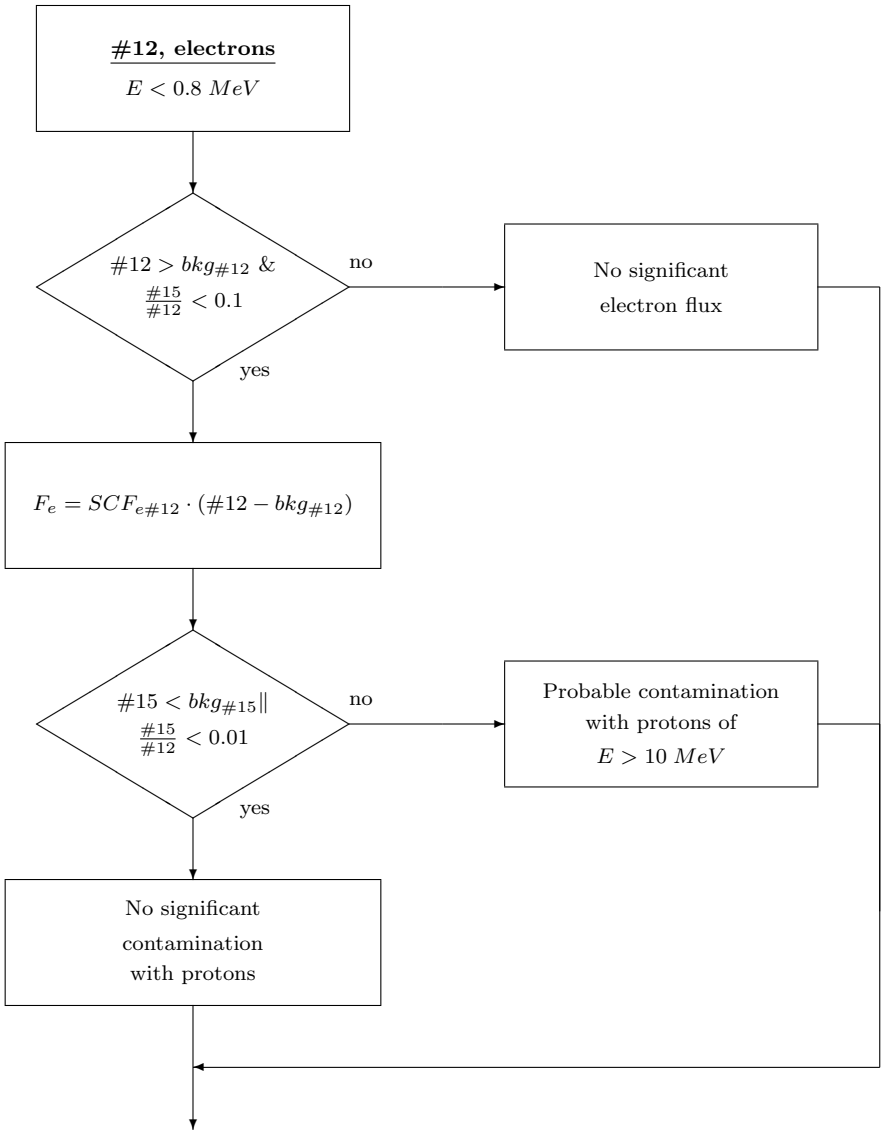
#12, electrons
$E < 0.8\ MeV$
$\#12 > bkg_{\#12}$ &
$\frac{\#15}{\#12} < 0.1$
no
No significant
electron flux
yes
$F_e = SCF_{e\#12} \cdot (\#12 - bkg_{\#12})$
$\#15 < bkg_{\#15}\|$
$\frac{\#15}{\#12} < 0.01$
no
Probable contamination
with protons of
$E > 10\ MeV$
yes
No significant
contamination
with protons

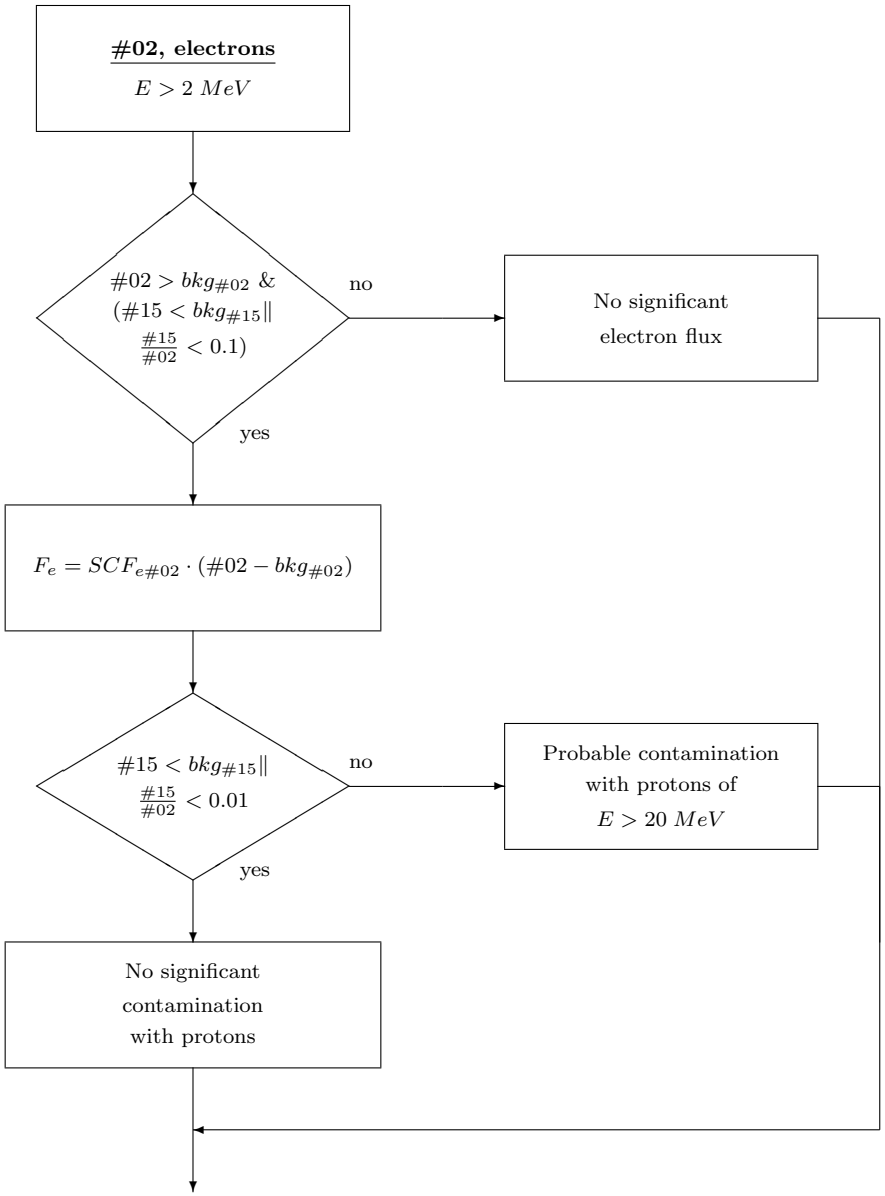
#02, electrons
$E > 2\ MeV$
$\#02 > bkg_{\#02}$ &
$(\#15 < bkg_{\#15} \| \frac{\#15}{\#02} < 0.1)$
no
No significant electron flux
yes
$F_e = SCF_{e\#02} \cdot (\#02 - bkg_{\#02})$
$\#15 < bkg_{\#15} \| \frac{\#15}{\#02} < 0.01$
no
Probable contamination with protons of $E > 20\ MeV$
yes
No significant contamination with protons

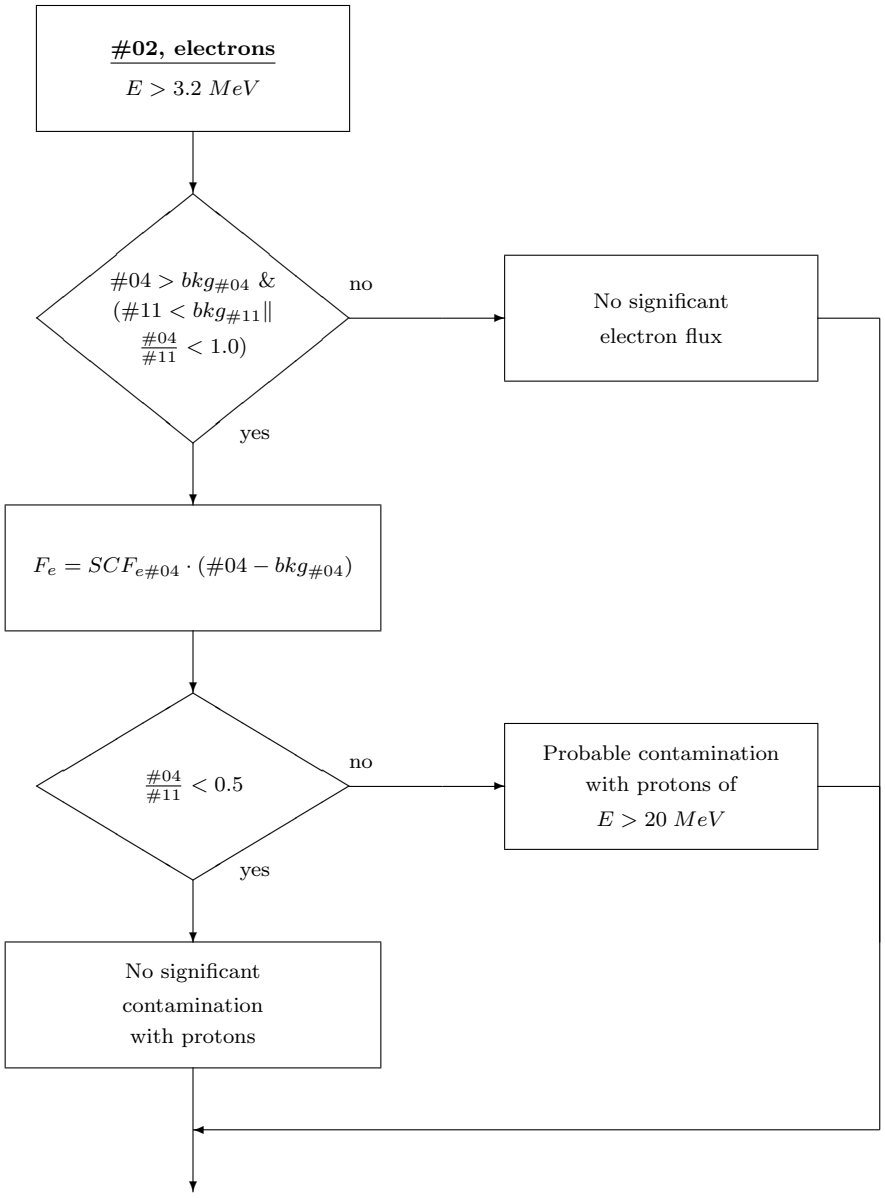
#02, electrons
$E > 3.2\ MeV$
$\#04 > bkg_{\#04}$ &
$(\#11 < bkg_{\#11} \|$
$\frac{\#04}{\#11} < 1.0)$
no
No significant
electron flux
yes
$F_e = SCF_{e\#04} \cdot (\#04 - bkg_{\#04})$
$\frac{\#04}{\#11} < 0.5$
no
Probable contamination
with protons of
$E > 20\ MeV$
yes
No significant
contamination
with protons

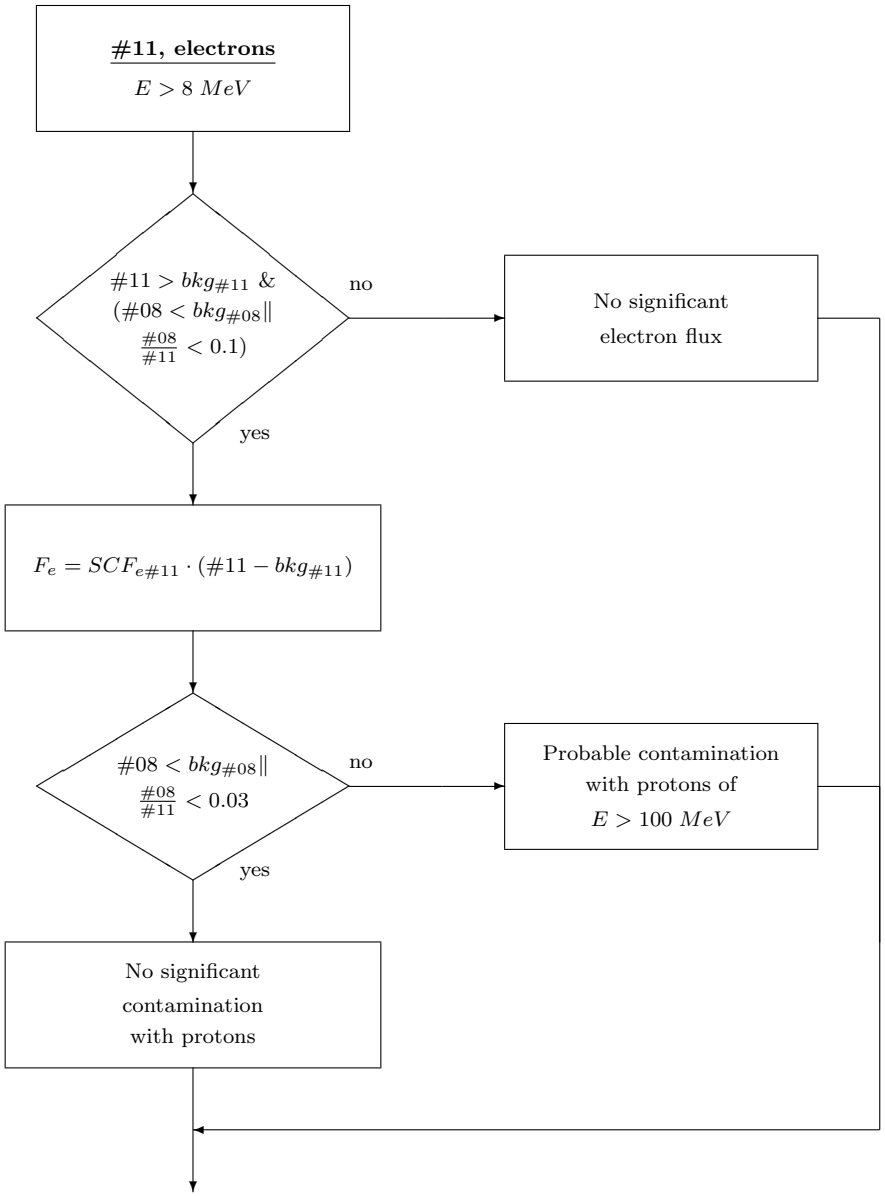
#11, electrons
$E > 8\ MeV$
$\#11 > bkg_{\#11}$ &
$(\#08 < bkg_{\#08} \| \frac{\#08}{\#11} < 0.1)$
no
No significant electron flux
yes
$F_e = SCF_{e\#11} \cdot (\#11 - bkg_{\#11})$
$\#08 < bkg_{\#08} \| \frac{\#08}{\#11} < 0.03$
no
Probable contamination with protons of $E > 100\ MeV$
yes
No significant contamination with protons

3.2 Parametrization of particle fluxes, Smooth functions

For this method equations (3), (4), and (5) are exploited to compute the set of spectral parameters α which best fit the measured counter values. In the current implementation this problem is solved with the program MINUIT.

This is currently the default method which is used to compute the energy spectra. For automated processing the spectral fit models are fixed. The proton spectral shape is modeled with a power law function and the electron spectrum with an exponential function. In order to guarantee good fit results, the automated processing is restricted to histograms with a minimum number of counts.

3.3 Parametrization of particle fluxes, Step function

The relation between the count rates and the flux levels $\{\overline{f_p}, \overline{f_e}\}$ of a step function approximation of the true particle spectra is given by the set of linear equations (7).

This Ansatz has already been used for the unfolding of REM data [*Bühler, 1996*] and has also been discussed in the context of SREM [*Bühler et al., 1998*].

The equations can be solved by a minimum non-negative least-squares method. However, the such obtained results tend to be unstable. A typical feature of the resulting flux levels is oscillation - bins with small values follow bins with large values. This is especially the case for low statistics histograms, where the relative statistical errors are large. With the conventional method of solving equations (7) this problem can be omitted by careful selection of the energy bins for each histogram individually.

In order to stabilize the procedure a regularization method was implemented which follows an algorithm described by *Höcker & Kartvelishvili* [1995]. The regularization consists in using some a priori information which puts additional constraints on the solution $\{\overline{f_p}, \overline{f_e}\}$.

Whereas the solution without regularization is obtained by minimizing

$$(\mathcal{RF} \times \{\overline{f_p}, \overline{f_e}\} - \overline{c})^T (\mathcal{RF} \times \{\overline{f_p}, \overline{f_e}\} - \overline{c}) = \min \tag{13}$$

(the conventional χ^2 minimization for linear systems) the regularization is achieved with an extra term

$$(\mathcal{RF} \times \{\overline{f_p}, \overline{f_e}\} - \overline{c})^T (\mathcal{RF} \times \{\overline{f_p}, \overline{f_e}\} - \overline{c}) + \tau \cdot (\mathcal{C} \times \{\overline{f_p}, \overline{f_e}\})^T (\mathcal{C} \times \{\overline{f_p}, \overline{f_e}\}) = \min \tag{14}$$

$\mathcal{C}$ is a matrix which defines the a priori condition and τ, the regularization parameter, determines the relative weight of this condition.

Besides $\mathcal{C}$ and τ also the number and width of the energy bins $E_{q,i}$ (see equation (6)) have to be chosen. For this study the proton energy range between 9 MeV and 500 MeV is split into 5 equally wide bins on a logarithmic scale and for the electrons the energy range between 0.5 MeV and 6.0 MeV is split into 3 bins.

As a first step the equations (7) are normalized and scaled to take into account the measurement errors and the large differences between the expected flux levels in the different energy bins.

$\{\overline{f_p}, \overline{f_e}\}$ is multiplied with a scaling matrix $\mathcal{H}^{-1}$ and both sides are multiplied with the covariance matrix $\mathcal{B}$ of the measured counts c_i. The modified equation (7) then comes out to be

$$\mathcal{B} \times \mathcal{RF} \times \mathcal{H} \times \mathcal{H}^{-1} \times \{\overline{f_p}, \overline{f_e}\} = \mathcal{B} \times \overline{c} \tag{15}$$

and can be written as

$$\mathcal{A} \times \overline{w} = \overline{b} \tag{16}$$

where $\mathcal{A} = \mathcal{B} \times \mathcal{RF} \times \mathcal{H}$, $\overline{w} = \mathcal{H}^{-1} \times \{\overline{f_p}, \overline{f_e}\}$, and $\overline{b} = \mathcal{B} \times \overline{c}$.

These normalized equations are solved for $\overline{w}$, which is used to compute $\{\overline{f_p}, \overline{f_e}\} = \mathcal{H} \times \overline{w}$. Here the covariance matrix $\mathcal{B}$ is assumed to be diagonal with $\mathcal{B}_{ii} = 1/\sqrt{c_i}$ and scaling matrix $\mathcal{H}$ is also diagonal with $\mathcal{H}_{ii} = 1/\sqrt{\sum_l (\mathcal{RF}_{li}^2)}$.

The a priori condition applied is the curvature of the spectrum, which is required to be small at all points of the spectrum. This does not force the solution to follow a given spectral shape, as in the case described in the previous section. But it tends to smoothen the result, and therefore suppresses unwanted oscillations.

For the discrete function $\overline{f}$ a representative value for the curvature γ_i at f_i can be computed with

$$\gamma_i = f_{i-1} - 2 \cdot f_i + f_{i+1} \tag{17}$$

$\mathcal{C}$ is accordingly

$$\mathcal{C} = \begin{pmatrix} 0 & 0 & 0 & 0 & 0 & 0 & 0 & 0 \\ 1 & -2 & 1 & 0 & 0 & 0 & 0 & 0 \\ 0 & 1 & -2 & 1 & 0 & 0 & 0 & 0 \\ 0 & 0 & 1 & -2 & 1 & 0 & 0 & 0 \\ 0 & 0 & 0 & 0 & 0 & 0 & 0 & 0 \\ 0 & 0 & 0 & 0 & 0 & 0 & 0 & 0 \\ 0 & 0 & 0 & 0 & 0 & 1 & -2 & 1 \\ 0 & 0 & 0 & 0 & 0 & 0 & 0 & 0 \end{pmatrix} \tag{18}$$

Note, that the curvature at the endpoints of the spectra can not be computed and therefore the elements of the corresponding rows in matrix $\mathcal{C}$ are all 0 (rows $1, 5, 6,$ and 8). There are four rows with 0s (four end points) because solution $\{\overline{f_p}, \overline{f_e}\}$ contains two independent spectra for protons and electrons.

The value of τ determines the relative importance between the χ^2-term in equation (14) (first term) and the regularization term. $\tau = 0$ is equivalent with the non-regularized situation and a very large τ puts more weight on the smoothness of the spectrum than on the goodness of fit measured by χ^2.

The method described in *Höcker & Kartvelishvili* [1995] for selection of the value of τ is suited for a large number of bins to fit and also requires some human evaluation. Since here the number of bins is small (8) and an automated processing is envisaged, this method needs to be adapted.

In *Höcker & Kartvelishvili* τ is computed as the square of a selected singular value s_k of the matrix $\mathcal{A} \times \mathcal{C}^{-1}$. The procedure to select the appropriate singular value and the justification for this method are detailed there. Here we use the simplified scheme

$$\tau = s_1^2 \cdot 10^{-7} \tag{19}$$

For histograms with good statistics, the singular values and thus also τ are small. For histograms with bad statistics the singular values are large and thus the regularization enforced.

With the given $\mathcal{C}$ and τ the set of normalized and regularized linear equations is solved with the method discussed in *Höcker & Kartvelishvili* [1995].

3.3.1 Examples

Figures 8 and 9 show some examples. Figure 8 contains examples with simulated histograms, with different relative contributions of protons and electrons. The black lines show the nominal spectra, the green lines the fit results with continuous functions and the magenta and orange crosses show the results of the fit with a step-like function - using the conventional method without regularization (magenta) and the new method with regularization.

Except for cases d) and e) the fit results of all methods are in relatively good agreement with the nominal functions. In case of the non-regularized fit however, some oscillations are visible (see protons in case b) and electrons in case c)) which do not occur with the regularized method. In cases d) and e), where the contribution of the protons dominates, the parameter fit fails to find the true electron spectrum. The regularized step function fit returns reasonable spectra even in these cases, however with relatively large uncertainty ranges.

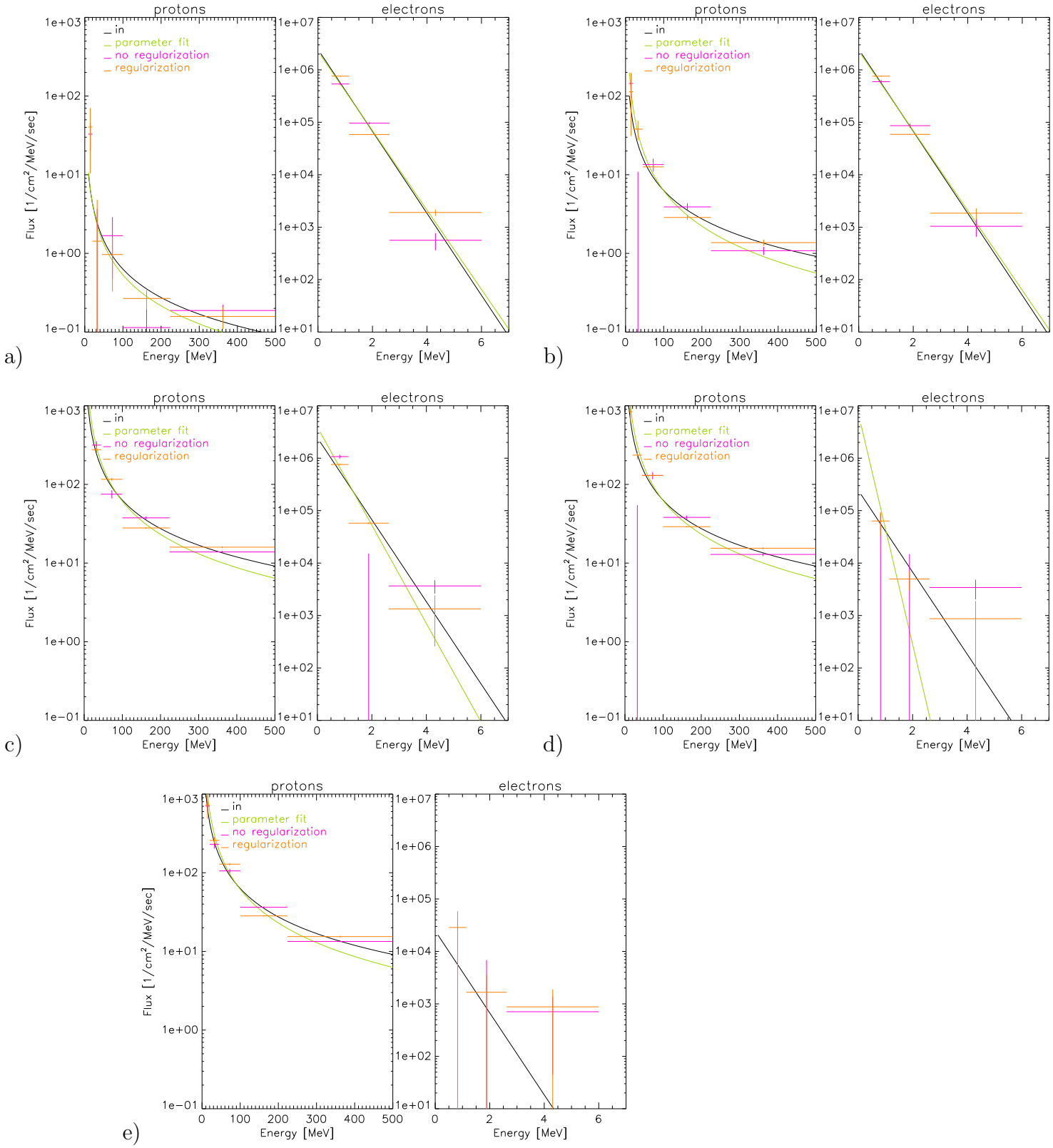

Figure 8: Exemplary fits of simulated histograms. The black lines show the nominal spectra (protons left panel, electrons right panel), the green line show the continuous function fit and the magenta and orange crosses show the fit results with the step function - without (magenta) and with (orange) regularization.

Figure 9 shows a few real examples from PROBA1/SREM. The first two examples (panels b) and c)) were measured in the outer electron belt (see vertical magenta lines in panel a)) and the third example d) was measured in the SAA. In b) and c) the parameter fit and the regularized step function fit for the electrons agree well. In these cases the proton contribution is negligible. In case d) the parameter fit and the regularized step function fit for the protons agree well. In this case the parameter fit returns no electron spectrum whereas the step function fit does find a small electron contribution. Whether the result of the step function fit in this case is correct is difficult to judge without other references. However, this case is typical for the measurements of PROBA1/SREM in the SAA and is probably similar to the simulated cases shown in panels d) and e) of figure 8, where the electron contribution is small compared to the proton contribution. Note, that in these cases the parameter fit happens to fail to find the true electron spectrum, whereas the regularized step function fit does return a reasonable electron spectrum.

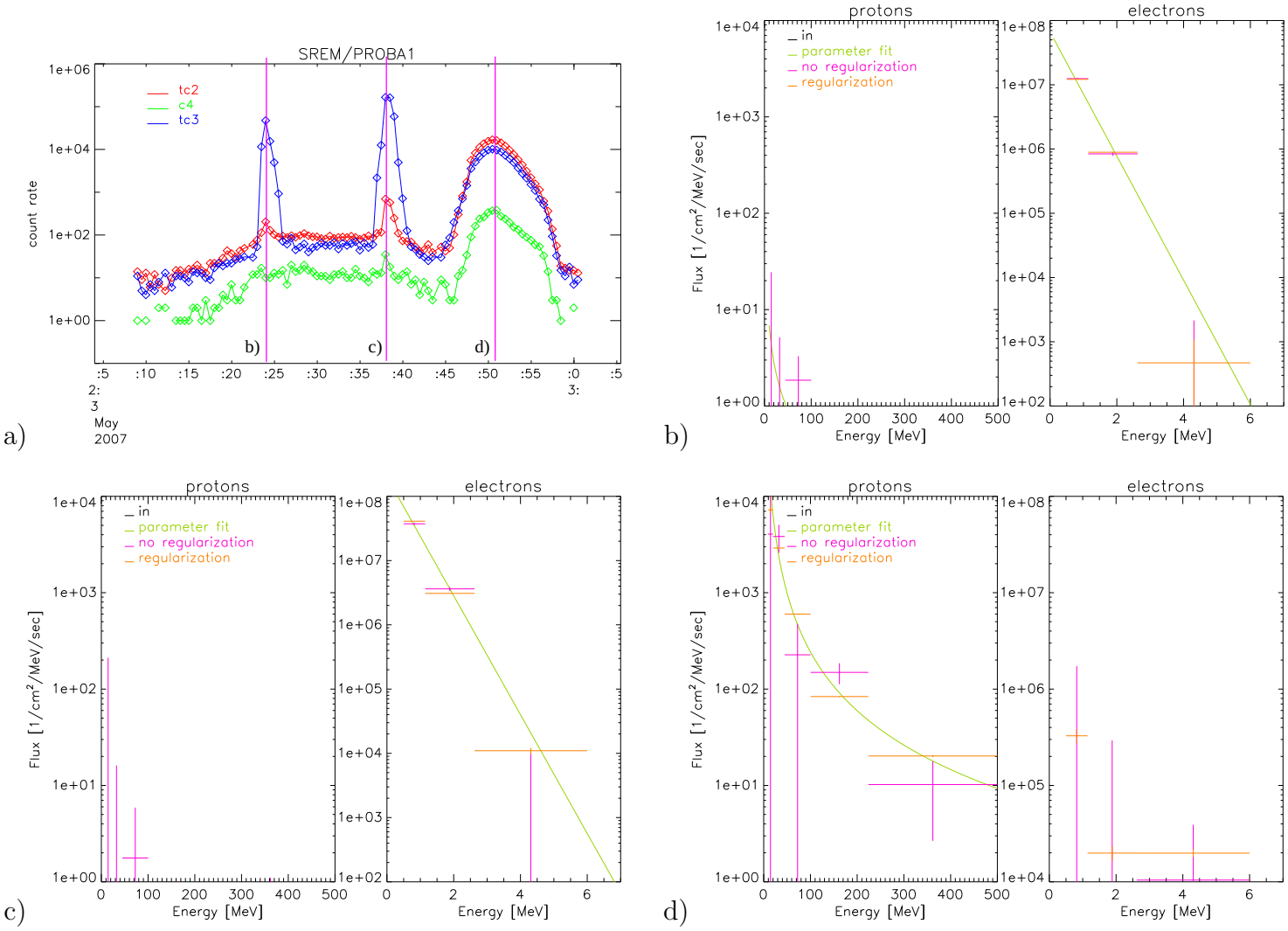

Figure 9: Same as figure 8 but for real data from PROBA1/SREM. The examples are from May 3, 2007, the period for which the count rates in counter tc2, c4, and tc3 are shown in panel a). Panel b) corresponds to the first peak of the tc3 count rate curve, panel c) to the second peak, panel d) to the third peak. b) and c) are in the outer electron belt, whereas d) is in the SAA.

4 Final remarks

- The SCF method is very attractive for automated processing of SREM data because of its simplicity. However, this method has two serious drawbacks
  - it is assumed, that only one particle species contributes to the counts, therefor measurements e.g. during solar events in the outer electron belt are difficult to unfold with this method
  - variations of the incident particle spectral shapes are not properly accounted for by this method
- Fitting the spectra with smooth functions is currently the routinely applied method. For protons a power law, and for electrons an exponential function is used. For measurements with sufficient counts, this method gives reliable information on the flux levels and also on the spectral hardness. The possible solutions are however restricted by the chosen spectral shapes which might lead to misleading results if the incident spectra are badly described by the chosen functions.
  For low statistics observations the result of this method can fail with a given set of initial fit parameter values. For automated processing therefor a lower limit on the count rate is imposed, leading to a cut-off of the unfolded spectra at low fluxes.
- The regularized step function fit combines nice features
  - proton and electron spectra are computed simultaneously
  - The resulting spectra are not restricted to a selected spectral model (although smooth spectral shapes are privileged by the method)

  The presented examples suggest, that both fitting methods provide similar results but that the step function fit might even be better in unfolding measurements with strongly different contributions of protons and electrons.
- In all cases it was assumed, that the particle fluxes are isotropic. In many real cases this is of course only a crude approximation (see e.g. [*Bühler et al., 1999*]).